Influences of Ferromagnetic Deflectors Between Layers of Superconducting Power Transmission Cables on Transport Current Losses

Chapter · October 2014

DOI: 10.1007/978-3-319-04681-5_40

2 authors:

Fedai inanır
Yildiz Technical University
37 PUBLICATIONS **192** CITATIONS

SEE PROFILE

Ahmet Cicek
Mehmet Akif Ersoy University
66 PUBLICATIONS **793** CITATIONS

SEE PROFILE

Metadata of the chapter that will be visualized online

Chapter Title	Influences of Ferromagnetic Deflectors Between Layers of Superconducting Power Transmission Cables on Transport Current Losses	
Copyright Year	2014	
Copyright Holder	Springer International Publishing Switzerland	
Corresponding Author	Family Name	**Cicek**
	Particle	
	Given Name	**Ahmet**
	Suffix	
	Division	Department of Physics, Faculty of Arts and Sciences
	Organization	Mehmet Akif Ersoy University
	Address	Campus 15100, Burdur, Turkey
	Email	ahmetcicek@mehmetakif.edu.tr
Author	Family Name	**Inanir**
	Particle	
	Given Name	**Fedai**
	Suffix	
	Division	Department of Physics, Faculty of Arts and Sciences
	Organization	Recep Tayyip Erdoğan University
	Address	53100, Rize, Turkey
	Email	inanir@ktu.edu.tr

Abstract

Alternating-current losses in two-layer power transmission cables constructed by type-II superconducting strips in the presence of ferromagnetic deflectors between the layers are numerically investigated. Each layer comprises 15 wires with rectangular cross section of 4 mm width and 2 μm height, while the inner and outer layer radii are 20 and 21 mm, respectively. Deflectors are composed of either non-magnetic or strongly ferromagnetic material, where the width and height of each is 5 mm and 80 μm, respectively. Losses are obtained through Finite-Element Method simulations with respect to amplitude of the applied current with 1 Hz frequency. Use of ferromagnetic deflectors increases the total alternating-current loss in the two layers considerably for small amplitudes, while the loss approaches that in non-magnetic case at amplitudes around the critical current. Individual layer losses are such that outer-layer loss is significantly larger, 2.5-fold at 1/16 of the critical current, for ferromagnetic deflectors, whereas they are almost identical in non-magnetic case at all amplitudes. Inner and outer wires are exposed to similar self magnetic fields of wires in non-magnetic case, while ferromagnetic deflectors accumulate magnetic field lines on themselves

and increase the losses in outer wires. The current profile is homogeneous except at the edges of the wires in the non-magnetic case, whereas homogeneity is disrupted for the outer wire in the case of ferromagnetic deflectors, such that current flow in the positive direction is confined to the central region.

Keywords (separated by “-”)	Two-layer superconducting cable - Ferromagnetic deflector - Alternating-current loss - Finite-element method

Influences of Ferromagnetic Deflectors Between Layers of Superconducting Power Transmission Cables on Transport Current Losses

40

Ahmet Cicek and Fedai Inanir

Abstract

Alternating-current losses in two-layer power transmission cables constructed by type-II superconducting strips in the presence of ferromagnetic deflectors between the layers are numerically investigated. Each layer comprises 15 wires with rectangular cross section of 4 mm width and 2 μm height, while the inner and outer layer radii are 20 and 21 mm, respectively. Deflectors are composed of either non-magnetic or strongly ferromagnetic material, where the width and height of each is 5 mm and 80 μm, respectively. Losses are obtained through Finite-Element Method simulations with respect to amplitude of the applied current with 1 Hz frequency. Use of ferromagnetic deflectors increases the total alternating-current loss in the two layers considerably for small amplitudes, while the loss approaches that in non-magnetic case at amplitudes around the critical current. Individual layer losses are such that outer-layer loss is significantly larger, 2.5-fold at 1/16 of the critical current, for ferromagnetic deflectors, whereas they are almost identical in non-magnetic case at all amplitudes. Inner and outer wires are exposed to similar self magnetic fields of wires in non-magnetic case, while ferromagnetic deflectors accumulate magnetic field lines on themselves and increase the losses in outer wires. The current profile is homogeneous except at the edges of the wires in the non-magnetic case, whereas homogeneity is disrupted for the outer wire in the case of ferromagnetic deflectors, such that current flow in the positive direction is confined to the central region.

Keywords

Two-layer superconducting cable • Ferromagnetic deflector • Alternating-current loss • Finite-element method

Introduction

Among promising applications of high-temperature superconductors (HTS) is power transmission. HTS power transmission cables generally operate at temperatures between 64 and 77 K. The most important advantages of these cables on conventional ones are the ability to transport high currents and their efficiency.

In evaluation of the efficiency of HTS cables, determination of alternating-current (AC) transport losses plays a central role. Primary factors affecting AC losses include (1) the number and dimensions of the wires composing a cable, (2) geometrical alignment of wires on cables and (3) the twist-pitch length.

A. Cicek (✉)
Department of Physics, Faculty of Arts and Sciences, Mehmet Akif Ersoy University, Campus 15100, Burdur, Turkey
e-mail: ahmetcicek@mehmetakif.edu.tr

F. Inanir
Department of Physics, Faculty of Arts and Sciences, Recep Tayyip Erdoğan University, 53100 Rize, Turkey
e-mail: inanir@ktu.edu.tr

I. Dincer et al. (eds.), *Progress in Exergy, Energy, and the Environment*,
DOI 10.1007/978-3-319-04681-5_40,

The critical current densities (J_c) of HTS cables depend heavily on the magnetic field distribution at elevated temperatures. In such power transmission cables, the total critical current density is higher than the sum of the corresponding densities of the strips forming the cable [7]. The reason for this lies in the fact that the variation in magnetic field distribution takes place in a more favorable manner, especially along the edges of an individual strip.

Ferromagnetic deflectors are successfully utilized in HTS coils and practical applications [6, 12]. It is reported that a correction in the critical current density (J_c) is required in strips coated by a ferromagnetic jacket [4]. The ferromagnetic material restrains coupling between the filaments within the superconductor [3]. This is expected to give rise to a decline in the transport AC losses in HTS cables. This is demonstrated by occupying the space between the filaments which inhibits the interaction between the filaments and facilitates decrease in AC losses [5]. Screening in HTS strips coated by ferromagnetic materials is also studied [1, 13]. Furthermore, influence of magnetization on AC transport losses in superconductors over a ferromagnetic substrate due to applied magnetic field is studied [9, 10]. It is reported that an important improvement in the performance of BiSCCO-2223 strips coated by a partially ferromagnetic material can be achieved [8]. Vojenčiak et al. [11] demonstrated both theoretically and experimentally that introduction of ferromagnetic deflectors in the space between the strips of a single-layer HTS cable gives rise to a reduction in AC losses.

Application of ferromagnetic deflectors between the layers of a two-layer HTS cable could also give rise to a reduction in AC transport losses in such cables. This work focuses on a numerical investigation on the influences of ferromagnetic deflectors introduced in the space between the HTS strips in a two-layer cable along the radial direction. The variation of transport current losses with respect to the applied current for deflectors with varying permeability is studied.

Cable Geometry and Computational Methods

The two-layer HTS cable geometry is depicted in Fig. 40.1. Each layer comprises $N = 30$ rectangular superconducting tapes with width and height as $w_{sc} = 4.0$ mm and $h_{sc} = 2.0$ μm, where the inner and outer layers are on circular arcs with $R_i = 20.0$ mm and $R_o = 21.0$ mm, respectively. The wire parameters are compatible with the standards set by American Superconductors Inc. The core of the cable is made of copper (Cu), whereas the space between the layers is filled with Kapton® dielectric. The ferromagnetic deflectors between the layers also possess a rectangular cross section with $w_T = 5.0$ mm and $h_T = 80.0$ μm, Fig. 40.1b.

The two-layer HTS cable in Fig. 40.1a possesses discrete azimuthal symmetry with respect to a unit of rotation by $\theta_C = 2\pi/30$ (12°), whereas the ferromagnetic deflectors, aligned on a circle with Radius $R_T = 20.5$ mm, are rotated by

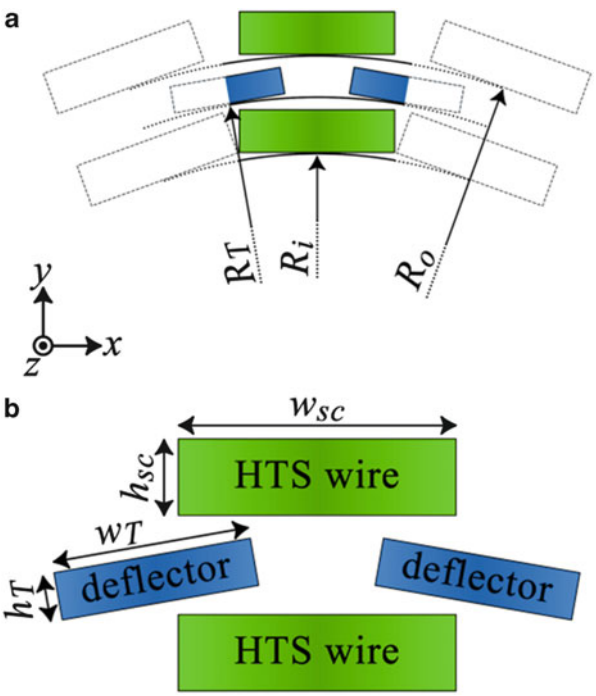

Fig. 40.1 Geometry of the two-layer HTS cable with ferromagnetic deflectors (**a**) and a close-up view of the wires and deflectors (**b**). Elements are not drawn to scale for clarity

$\theta_T = \theta_C/2 = 2\pi/62$ (5.8°) with respect to the wires. Due to the above-mentioned symmetry, the problem in two dimensions (2D) is solved through the Comsol MultiPhysics® package with AC/DC module, which is a commercial implementation of the Finite Element Method (FEM), by only considering the periodic element in Fig. 40.1a. Thus, the two wires and halves of the deflectors, which are depicted by the filled rectangles with solid borders, are considered in computations, Fig. 40.1a.

The HTS wires are composed of second-generation yttrium barium copper oxide (YBCO) superconductors, whereas the deflectors are either non-magnetic or strongly ferromagnetic with relative permeability of $\mu_r = 1.0$ and 5,000, respectively. The magnetic flux dependence of the ferromagnetic deflectors is assumed as $B = \mu_0\mu_r H$ and ferromagnetic losses are ignored. The influence of the substrate is neglected for simplicity, so that it is not depicted in Fig. 40.1a. Moreover, twisting of the wires along the z direction is also not taken into account. The choice of geometrical and physical parameters is to facilitate a comparison between other possible configurations of the cable with respect to the use of ferromagnetic material.

In FEM simulations, an alternating current with a frequency of f is applied along the z direction and the component of the vector potential along this direction (A_z) is treated as the independent variable. The rotational of the vector potential yields magnetic flux density. The critical current for each wire, which is calculated through an integration of the critical current density (J_c) over the cross-sectional area (A_{SC}) of the wire on the xy-plane,

$$I_c = \int_{A_{SC}} J_c \, dA_{SC} \tag{40.1}$$

is taken as $I_c = 80$ A. Dependence of I_c on magnetic flux density and position, which may be important in case of wires with circular cross-sections, is ignored. The current is sinusoidal with $I(t) = I_{max}.\sin(2\pi ft)$, where I_{max} is its amplitude with respect to I_c and $f = 1$ Hz.

The boundary condition for addressing the cable geometry in Fig. 40.1a considers the vector potential at an arbitrary position r due to an HTS wire in Fig. 40.1b as

$$A_r = -\frac{\mu_0 I}{2\pi}\left(\ln\left(\frac{r}{R_i + h_{SC}}\right) + \ln\left(\frac{r}{R_o + h_{SC}}\right) + 2\right) \tag{40.2}$$

Besides, the azimuthal boundary condition exploits continuity of the normal component of the magnetic field. The superconducting current density in computations can be written as

$$j_{sc,z}(x,y) = J_c \tanh\left(\frac{A_p(x,y) - (A_z(x,y) + \nabla V)}{A_n}\right) \tag{40.3}$$

where $A_p(x,y)$ is the distribution of $A_z(x,y)$ in the previous step in the time march of simulations, whereas A_n is the scaling parameter which adjusts the sharpness of the translations between the region in superconductor with positive and negative current densities and ∇V is the scalar potential. By numerically solving Ampere's Law in combination with Eqs. (40.2) and (40.3), the distributions of $j_{sc,z}$ and $\mathbf{E} = -\partial\mathbf{A}/\partial t - \nabla V$ over a wire's cross-section are calculated and AC loss, Q (J/m), in each wire is obtained, in turn, by:

$$Q = \int_{A_{sc}} \mathbf{E} \cdot \mathbf{j} \, dA_{sc} \tag{40.4}$$

Results and Discussion

Variation of the total AC transport loss (Q_e) of the HTS cable on each periodic element in Fig. 40.1a with respect to the applied current amplitude is depicted in the log–log scale in Fig. 40.2. In computations I_{max} is set to eight different values ranging from 5.0 to 75.0 A (I_c/16 to 15I_c/16). Q_e is calculated as the sum of the losses in inner (Q_i) and outer (Q_o) layers.

Figure 40.2 demonstrates that use of strongly ferromagnetic deflectors significantly increases Q_e, while the discrepancy between the two materials vanishes for large current amplitudes close to I_c. The losses increase almost linearly in Fig. 40.2 for $I_{max} < I_c/2$, whereas the increase is slightly steeper at higher amplitudes. The calculated losses for $\mu_r = 1.0$ are

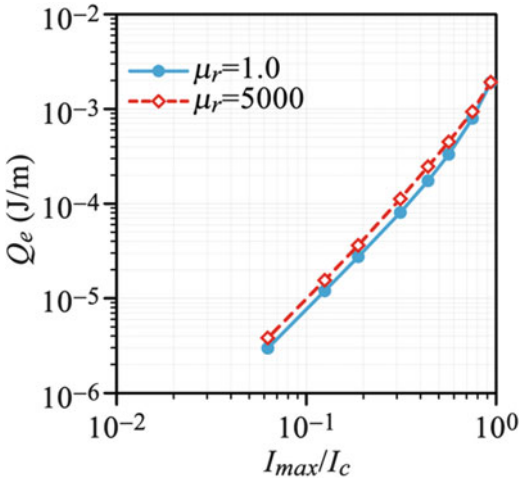

Fig. 40.2 Variation of total AC transport loss on each periodic element with respect to the applied current amplitude for non-magnetic and strongly ferromagnetic deflectors

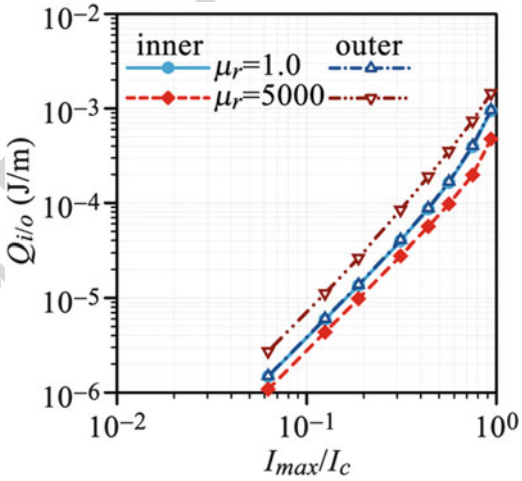

Fig. 40.3 Comparison of individual AC transport losses on the inner and outer layers of the HTS cable for non-magnetic and strongly ferromagnetic deflectors

2.98×10^{-6}, 1.74×10^{-4} and 1.91×10^{-3} J/m for $I_{max} = 5.0$ A ($I_c/16$), 35.0 A ($7I_c/16$), and 75.0 A ($15I_c/16$), respectively. Corresponding losses for $\mu_r = 5{,}000$ are 3.82×10^{-6}, 2.47×10^{-4} and 1.93×10^{-3} J/m, respectively. These values are 28.2, 41.4 and 0.8 % higher than the corresponding values in the $\mu_r = 1.0$ case.

To elucidate the loss mechanism due to the presence of deflectors, individual losses on each layer should be considered. Figure 40.3 depicts the variation of Q_i and Q_o with respect to I_{max}. In case of $\mu_r = 1.0$, Q_i and Q_o are almost equal to each other (and thus to $Q_e/2$), as expected. In contrast, a significant discrepancy is observed for $\mu_r = 5{,}000$, where Q_i is considerably smaller at all I_{max} values. In fact, Q_i is also smaller than the corresponding value for the non-magnetic deflector case. The value of Q_i and Q_o are 1.1×10^{-6} and 2.7×10^{-6} J/m, respectively, such that Q_o is 145.4 % higher than Q_i, at $I_{max} = 5.0$ A ($I_c/16$) for the ferromagnetic deflectors. The corresponding value for non-magnetic deflectors is 1.5×10^{-6} J/m, which is 35.8 % larger than the Q_i value at the same amplitude for the ferromagnetic case. Q_i and Q_o for $\mu_r = 5{,}000$ becomes 5.6×10^{-5} and 1.9×10^{-4} J/m, respectively at $I_{max} = 35.0$ A ($7I_c/16$), that is Q_o is almost fourfold higher at amplitudes around $I_c/2$. At the highest amplitude ($15I_c/16$), the corresponding values are calculated as 4.7×10^{-4} and 1.5×10^{-3} J/m, respectively. Although presence of ferromagnetic deflectors increases the total AC transport loss, the loss in the inner layer of the cable can be tuned by modifying the deflector parameters. This can particularly be important in technological applications in order to reduce process and cooling-down costs [2].

How the relative permeability of deflectors influences AC losses is closely related to how they manipulate the magnetic field distribution around the HTS wires. Figure 40.4 presents distribution of the equi-potential lines of the magnetic vector potential (A_z) for non-magnetic and strongly ferromagnetic deflectors at an instant, at which the instantaneous current on a wire is $I(t) = 18.5$ A, of the sine-wave cycle of the applied current with $I_{max} = 75.0$ A.

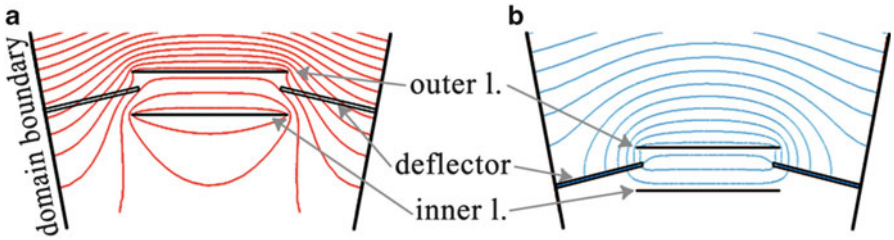

Fig. 40.4 Distribution of the equi-potential lines of the magnetic vector potential (A_z) around the wires for $\mu_r = 1.0$ (**a**) and 5,000 (**b**) at an instant of the applied sinusoidal current such that the instantaneous current takes a moderate value (18.5 A)

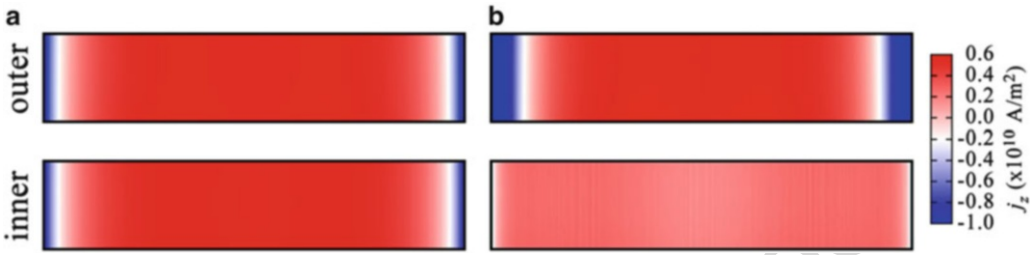

Fig. 40.5 Distribution of current amplitude over the inner (*lower*) and outer (*upper*) wires of the HTS wire for non-magnetic (**a**) and strongly ferromagnetic (**b**) deflectors at an instant of the applied sinusoidal current such that the instantaneous current takes a moderate value (18.5 A)

Non-magnetic deflectors do not affect the magnetic field lines due to current distributions in the wires as expected, Fig. 40.4a. Besides, the wires on the inner and outer layers are exposed to similar self-fields. Thus, Q_i and Q_o for $\mu_r = 1.0$ in Fig. 40.3 are almost equal. On the other hand, strongly ferromagnetic deflectors both trap and concentrate field lines on themselves, Fig. 40.4b. Moreover, the inner layer is exposed to its self-field to a lesser extent in this case. This is the reason behind the fact that Q_i for the ferromagnetic deflectors is smaller than both Q_o in the same configuration and the corresponding Q_i for non-magnetic deflectors, as seen in Fig. 40.3. Moreover, the normal component of the magnetic field is more dominant at the edges of the outer wire for $\mu_r = 5{,}000$. The above facts indicate that current distributions in the wires are affected by the presence of the ferromagnetic deflectors, as depicted in Fig. 40.5.

Figure 40.5a depicts that current flow is homogeneous in the interiors of both wires, while higher current amplitudes close to I_c are confined to the edges parallel to y direction in case of $\mu_r = 1.0$. Furthermore, the current distribution is almost identical in inner and outer wires, Fig. 40.5a. On the other hand, the situation is quite different in case of $\mu_r = 5{,}000$, as depicted in Fig. 40.5b. The current flow is more homogeneous in the inner wire, lower part of Fig. 40.5b, than in the case of non-magnetic deflectors. For this wire, the high current flow at the edge is confined to a smaller area. However, the region expands more into the wire along x direction in the outer wire, upper part of Fig. 40.5b. This, in turn, indicates that magnetic field penetrates deeper into the outer wire in case of ferromagnetic deflectors. The current distribution patterns in Fig. 40.5 are consistent with distribution of magnetic field lines in Fig. 40.4.

Conclusion

Alternating-current transport losses in two-layer high-temperature superconducting cables accompanied by ferromagnetic deflectors are numerically studied through FEM simulations. Presence of ferromagnetic deflectors with relative permeability as high as 5,000, located in the space between the layers and rotated by half the unit angle of rotation due to discrete azimuthal symmetry of the cable, increases the total loss relative to the case of non-magnetic deflectors. The increase in the total loss is due mainly to the increased self-magnetic field around the outer-layer wires, whereas the ferromagnetic deflectors concentrating magnetic field lines on themselves lead to a reduction in the individual losses of inner-layer wires. This fact can be utilized in tuning the losses in the inner layers of multi-layer cables to reduce both operation and cooling-down costs. In consistent with the distribution of magnetic field lines due to self-fields of the wires in the existence of ferromagnetic deflectors, the current flow is largely homogeneous in the inner-layer wires, while the region of high current flow expands more into the outer-layer wires.

Acknowledgments This study is supported by The Scientific and Technological Research Council of Turkey (TÜBİTAK) under the grant number 110T876.

References

1. Farinon S, Fabbricatore P, Gömöry F, Greco M, Seiler E (2005) Modeling of current density distributions in critical state by commercial FE codes. IEEE Trans Appl Supercond 15(2):2867–2870
2. Gerhold J, Tanaka T (1998) Cryogenic electrical insulation of superconducting power transmission lines: transfer of experience learned from metal superconductors to high critical temperature superconductors. Cryogenics 38(11):1173–1188
3. Glowacki BA, Majoros M (2000) A method for decreasing transport ac losses in multifilamentary and multistrip superconductors. Supercond Sci Technol 13(7):971–973
4. Kovác P, Hušek I, Melišek T, Ahoranta M, Šouc J, Lehtonen J, Gömöry F (2003) Magnetic interaction of an iron sheath with a superconductor. Supercond Sci Technol 16(10):1195–1201
5. Majoros M, Sumption MD, Collings EW (2009) Transport AC loss reduction in striated YBCO coated conductors by magnetic screening. IEEE Trans Appl Supercond 19(3):3352–3355
6. Pardo E, Šouc J, Vojenčiak M (2009) AC loss measurement and simulation of a coated conductor pancake coil with ferromagnetic parts. Supercond Sci Technol 22(7):075007
7. Rostila L, Söderlund L, Mikkonen R, Lehtonen J (2007) Modelling method for critical current of YBCO tapes in cable use. Physica C Supercond Appl 467(1–2):91–95
8. Safran S, Vojenčiak M, Gencer A, Gömöry F (2010) Critical current and AC loss of DI-BSCCO tape modified by the deposition of ferromagnetic layer on edges. IEEE Trans Appl Supercond 20(5):2294–2300
9. Seiler E, Gömöry F (2006) Modelling of the flux penetration into a superconducting strip with magnetic sheath. J Phys Conf Ser 43:9–13
10. Suenaga M, Iwakuma M, Sueyoshi T, Izumi T, Mimura M, Takahashi Y, Aoki Y (2008) Effects of a ferromagnetic substrate on hysteresis losses of a $YBa_2Cu_3O_7$ coated conductor in perpendicular ac applied magnetic fields. J Phys Conf Ser 97:012025
11. Vojenčiak M, Šouc J, Gömöry F (2011) Critical current and AC loss analysis of a superconducting power transmission cable with ferromagnetic diverters. Supercond Sci Technol 24(7):075001
12. Wen H, Bailey W, Goddard K, Al-Mosawi M, Beduz C, Yang Y (2009) Performance test of a 100 kW HTS generator operating at 67 K–77 K. IEEE Trans Appl Supercond 19(3):1652–1655
13. Yampolskii SV, Genenko YA, Rauh H (2007) Penetration of an external magnetic field into a multistrip superconductor/soft-magnet heterostructure. Physica C Supercond Appl 460–462(2):1262–1263

Author Queries

Chapter No.: 40 319936_1_En

Query Refs.	Details Required	Author's response
AU1	"Ahmet Cicek" has been set as the corresponding author. Please check and advise if correct.	
AU2	Please note that the phrase "Color online" has been removed as there is no explanation for color in the caption of Figs. 40.1–40.5.	